発表者氏名	論文タイトル名	発表誌名	巻号	ページ	出版年
Ueda M, Ota J, Yamashita Y, Choi YL, Ohki R, Wada T, Koinuma K, Kano Y, Ozawa K and Mano H	DNA microarray analysis of stage progression mechanism in myelodysplastic syndrome	Br J Haematol	123(2)	288-296	2003
Suzuki N, Nakamura S, Mano H and Kozasa T	Galpha 12 activates Rho GTPase through tyrosine-phosphorylated leukemia-associated RhoGEF	Proc Natl Acad Sci USA	100(2)	733-738	2003
Ota J, Yamashita Y, Okawa K, Kisanuki H, Fujiwara S, Ishikawa M, Choi YL, Ueno S, Ohki R, Koinuma K, Wada T, Compton D, Kadoya T and Mano H	Proteomic analysis of hematopoietic stem cell-like fractions in leukemic disorders	Oncogene	22(36)	5720-5728	2003
Oshima Y, Ueda M, Yamashita Y, Choi YL, Ota J, Ueno S, Ohki R, Koinuma K, Wada T, Ozawa K, Fujimura A and Mano H	DNA microarray analysis of hematopoietic stem cell-like fractions from individuals with the M2 subtype of acute myeloid leukemia	Leukemia	17(10)	1990-1997	2003
Ohmine K, Nagai T, Tarumoto T, Miyoshi T, Muroi K, Mano H, Komatsu N, Takaku F and Ozawa K	Analysis of Gene Expression Profiles in an Imatinib-Resistant Cell Line, KCL22/SR	Stem Cells	21(3)	315-321	2003
Ohki R, Yamamoto K, Ueno S, Mano H, Ikeda U and Shimada K	Effects of Olmesartan, an Angiotensin II Receptor Blocker, on Mechanically-Modulated Genes in Cardiac Myocytes	Cardiovasc Drugs Ther	17(3)	231-236	2003
Ogata Y, Takahashi M, Ueno S, Takeuchi K, Okada T, Mano H, Ookawara S, Ozawa K, Berk BC, Ikeda U, Shimada K and Kobayashi E:.:,	Antiapoptotic Effect of Endothelin-1 in Rat Cardiomyocytes In Vitro	Hypertension	41(5)	1156-1163	2003
Horwood NJ, Mahon T, McDaid JP, Campbell J, Mano H, Brennan FM, Webster D and Foxwell BM	Bruton's tyrosine kinase is required for lipopolysaccharide-induced tumor necrosis factor alpha production	J Exp Med	197(12)	1603-1611	2003
Oshima Y, AND Fujimura A	Function of a conserved residue in the amino terminal alpha-helix of four helical bundle cytokines.	Cytokine	24(1-2)	36-45	2003

発表者氏名	論文タイトル名	発表誌名	巻号	ページ	出版年
Oshima Y, AND Fujimura A	Analysis of 3'/5' Ratio of Actin and Glyceraldehyde-3-Phosphate Dehydrogenase (GAPDH).	Genome Informatics 2003	14	472-473	2003
Oshima Y, Kurokawa S, Tokue A, Mano H, Saito K, Suzuki M, Imai M AND Fujimura A	Primary cell preparation and genome-wide gene expression analysis of human renal tubular cells,	Toxicogenomics International Forum 2003	2003	82-83	2003
Tatsuo M, Atsushi M, Akihiko T	Quantitative Analysis of Thymidine Phosphorylase and Dihydropyrimidine Dehydrogenase in Renal Cell Carcinoma	Oncology	65(2)	125-131	2003
Tatsuo M, Atsushi M, Shinsuke k, Akihiko T	Forced Expression of Cytidine Deaminase Confers Sensitivity to Capecitabine	Oncology	65(3)	267-274	2003

健康危険情報

なし

厚生労働省科学研究費補助金

化学物質リスク研究事業

プライマリーヒト細胞を用いた化学物質曝露・遺伝子発現に関する研究(H15-化学-001)

平成15年度～17年度　総合研究報告書

主任研究者　藤村　昭夫

平成 18(2006)年 4 月

2/2 冊

Oncogene (2006) 25, 139–146

www.nature.com/onc

SHORT COMMUNICATION

Epigenetic silencing of *AXIN2* in colorectal carcinoma with microsatellite instability

K Koinuma[1,2], Y Yamashita[1], W Liu[3], H Hatanaka[1], K Kurashina[1,2], T Wada[1], S Takada[1], R Kaneda[1], YL Choi[1], S-I Fujiwara[1], Y Miyakura[2], H Nagai[2] and H Mano[1,4]

[1]Division of Functional Genomics, Jichi Medical School, Tochigi, Japan; [2]Department of Surgery, Jichi Medical School, Tochigi, Japan; [3]Division of Experimental Pathology, Mayo Clinic and Mayo Medical School, Rochester, MN, USA and [4]CREST, Japan Science and Technology Agency, Saitama, Japan

Mutation or epigenetic silencing of mismatch repair genes, such as *MLH1* and *MSH2*, results in microsatellite instability (MSI) in the genome of a subset of colorectal carcinomas (CRCs). However, little is yet known of genes that directly contribute to tumor formation in such cancers. To characterize MSI-dependent changes in gene expression, we have now compared transcriptomes between fresh CRC specimens positive or negative for MSI ($n = 10$ for each) with the use of high-density oligonucleotide microarrays harboring >44 000 probe sets. Correspondence analysis of the expression patterns of isolated MSI-associated genes revealed that the transcriptome of MSI$^+$ CRCs is clearly distinct from that of MSI$^-$ CRCs. Such MSI-associated genes included that for AXIN2, an important component of the WNT signaling pathway. *AXIN2* was silenced, apparently as a result of extensive methylation of its promoter region, specifically in MSI$^+$ CRC specimens. Forced expression of *AXIN2*, either by treatment with 5′-azacytidine or by transfection with *AXIN2* cDNA, resulted in rapid cell death in an MSI$^+$ CRC cell line. These data indicate that epigenetic silencing of *AXIN2* is specifically associated with carcinogenesis in MSI$^+$ CRCs.
Oncogene (2006) **25,** 139–146. doi:10.1038/sj.onc.1209009; published online 10 October 2005

Keywords: epigenetics; colorectal carcinoma; microsatellite instability; AXIN2; MLH1

Colorectal carcinoma (CRC) is one of the leading causes of cancer death in humans. Evidence indicates the existence of two major types of genomic instability in CRCs: chromosomal instability and microsatellite instability (MSI) (Lengauer *et al.*, 1998). Whereas chromosomal instability is associated with an abnormal DNA content (such as aneuploidy), inactivation of the tumor suppressor gene *TP53*, and activation of oncogenes (Kinzler and Vogelstein, 1996), MSI is associated with defects in DNA mismatch repair (MMR) that result in frameshift mutations in microsatellite repeats and thereby affect the structure of genes containing such repeats (Ionov *et al.*, 1993).

Although germline mutations of MMR genes have been detected in the genome of individuals with hereditary nonpolyposis colorectal cancer (Fishel *et al.*, 1993; Bronner *et al.*, 1994; Papadopoulos *et al.*, 1994), many sporadic CRCs positive for MSI are associated with epigenetic silencing of nonmutated MMR genes (Toyota *et al.*, 1999; Miyakura *et al.*, 2001). MSI$^+$ CRCs are characterized by specific clinicopathologic features and gene mutations. They occur with a higher frequency in women than in men, develop in the right side of the colon, and manifest a mucinous or poorly differentiated histopathology. Many of the CpG dinucleotides within the promoter region of the MMR gene *MLH1* are methylated (Cunningham *et al.*, 1998; Veigl *et al.*, 1998) and the *BRAF* gene frequently contains activating mutations (Koinuma *et al.*, 2004) in MSI$^+$ CRCs. Multiple genomic fragments have been found to be methylated in such CRCs (Toyota *et al.*, 1999), and an entity of CRC with a CpG island methylator phenotype has been proposed (Issa, 2004). The repertoire of genes that become methylated specifically in CRCs positive for *MLH1* methylation has remained uncharacterized, however.

To characterize directly the transcriptome specifically associated with MSI$^+$ CRC, we have now compared transcriptomes between fresh CRC specimens with or without MSI. Unexpectedly, we found that the expression of *AXIN2*, which encodes a component of the WNT signaling pathway, was markedly suppressed among the former tumors. CpG sequences within the *AXIN2* promoter were revealed to be extensively methylated in such CRCs. Forced expression of *AXIN2* inhibited cell proliferation in an MSI$^+$ CRC cell line, indicating that loss of *AXIN2* transcription is directly associated with carcinogenesis in MSI$^+$ CRCs.

To identify genes whose expression is specifically altered in MSI$^+$ CRCs, we first compared the transcriptomes of CRCs with or without MSI. A total of 248 consecutive cases of CRC were examined for MSI status

Correspondence: Professor H Mano, Division of Functional Genomics, Jichi Medical School, 3311-1 Yakushiji, Kawachigun, Tochigi 329-0498, Japan.
E-mail: hmano@jichi.ac.jp
Received 28 April 2005; revised 7 July 2005; accepted 13 July 2005; published online 10 October 2005

as well as for methylation of the promoter region of *MLH1* (Koinuma *et al.*, 2004). Most ($n=213$) of the cancer specimens were MSI$^-$, with the remainder ($n=35$) being positive for MSI. To compare the transcriptomes of these two subtypes of CRC, we randomly selected 10 specimens from each group and subjected them to gene expression profiling with microarrays (Affymetrix GeneChip HGU133) that harbor >44 000 probe sets. The clinical characteristics of the patients whose CRC specimens were subjected to microarray analysis are summarized in Table 1.

To exclude transcriptionally silent genes from our analyses, we first chose probe sets that received the 'Present' call from Microarray Suite 5.0 (Affymetrix) in at least 10% ($n=2$) of the samples. Two-way hierarchical clustering (Alon *et al.*, 1999) of the 20 patients based on the expression profiles of the isolated 21 888 probe sets failed to separate those with MSI$^+$ CRC from those with MSI$^-$ CRC (data not shown). We therefore attempted to identify 'MSI-associated probe sets' whose expression intensities differed significantly (Student's *t*-test, $P<0.001$) between the two classes and whose effect size (absolute difference in mean expression level) was $\geqslant 50$ U. Two-way clustering analysis with the 24 probe sets that fulfilled both these criteria clearly separated the individuals of the two clinical classes (Figure 1a). The distinct transcriptomes of the two classes were also confirmed by correspondence analysis (Fellenberg *et al.*, 2001), which reduced the complexity of the gene expression patterns from 24 to three dimensions. Projection of the study subjects into a virtual three-dimensional space based on their calculated coordinates revealed that the MSI$^+$ specimens were positioned apart from the MSI$^-$ ones (Figure 1b). These data indicate that the two classes of CRC possess distinct gene expression profiles, or 'molecular signatures', and they also suggest the feasibility of gene expression-based differential diagnosis of the two CRC subtypes.

Table 1 Clinical characteristics of the study subjects enrolled in microarray analysis

Patient ID	*Age (years)*	*Sex*	*MSI status*	MLH1 *methylation*	BRAF *gene*	KRAS2 *gene*	*Tumor site*	*Dukes stage*	*Pathology*	AXIN2 *methylation*
225	83	Female	Positive	Yes	Mutant	Wild	Proximal	C	Well	Yes
263	86	Female	Positive	Yes	Mutant	Wild	Proximal	C	Mod	Yes
280	83	Female	Positive	Yes	Mutant	Wild	Proximal	C	Well	Yes
305	74	Male	Positive	Yes	Mutant	Wild	Proximal	B	Sig	No
318	76	Female	Positive	Yes	Mutant	Wild	Proximal	B	Well	Yes
336	68	Male	Positive	Yes	Mutant	Wild	Proximal	B	Muc	No
413	69	Female	Positive	Yes	Mutant	Wild	Proximal	A	Well	No
416	76	Female	Positive	Yes	Mutant	Wild	Proximal	B	Muc	No
433	54	Female	Positive	Yes	Wild	Wild	Proximal	D	Well	Yes
479	74	Female	Positive	Yes	Mutant	Wild	Proximal	B	Mod	No
238	74	Male	Negative	No	Wild	Mutant	Distal	A	Well	No
249	62	Male	Negative	No	Wild	Wild	Proximal	B	Well	No
278	73	Male	Negative	No	Wild	Wild	Proximal	C	Well	No
295	71	Female	Negative	No	Wild	Mutant	Proximal	C	Well	No
298	70	Male	Negative	No	Wild	Mutant	Proximal	D	Well	No
307	80	Female	Negative	No	Wild	Wild	Proximal	C	Mod	No
308	62	Male	Negative	No	Wild	Wild	Distal	B	Mod	No
319	53	Female	Negative	No	Wild	Wild	Distal	A	Well	No
419	45	Female	Negative	No	Wild	Mutant	Proximal	D	Muc	No
426	42	Female	Negative	No	Wild	Wild	Proximal	C	Well	No

Well = well-differentiated adenocarcinoma; Mod = moderately differentiated adenocarcinoma; Sig = signet ring cell adenocarcinoma; Muc = mucinous adenocarcinoma. Methylation of *AXIN2* promoter region was determined by COBRA method.

Figure 1 Comparison of transcriptomes between CRCs positive or negative for MSI. **(a)** Subject tree generated by two-way clustering analysis with 24 probe sets that contrasted the two clinical conditions ($P<0.001$; effect size, $\geqslant 50$ U). Tumor samples were obtained from individuals with sporadic CRC who underwent surgical treatment at Jichi Medical School Hospital. Written informed consent was obtained from all patients, and the present study was approved by the ethics committee of Jichi Medical School. Microsatellite stability was determined by analysis of nine microsatellite repeat loci (three dinucleotide repeats and six mononucleotide repeats) as described previously (Miyakura *et al.*, 2001), and MSI status was stratified according to the criteria of the National Cancer Institute workshop (Boland *et al.*, 1998). Total RNA was extracted from ~100 mg of tissue, and was used in the hybridization experiments with GeneChip HGU133 A&B microarrays (Affymetrix), which harbor >44 000 probe sets corresponding to ~33 000 human genes, as described previously (Ohki-Kaneda *et al.*, 2004). The mean expression intensity of the internal positive control probe sets (http://www.affymetrix.com/support/technical/mask_files.affx) on the microarrays was set to 500 units (U) in each hybridization, and the fluorescence intensity of each probe set was normalized accordingly. All normalized array data are available at the Gene Expression Omnibus website (http://www.ncbi.nlm.nih.gov/geo) under the Accession Number GSE2138. Each column corresponds to a separate sample (MSI$^-$, green; MSI$^+$, red), and each row to a probe set whose expression is color-coded according to the indicated scale. Gene symbols are shown on the right; 225541_at, 226545_at, and 242414_at are expressed sequence tag IDs designated by Affymetrix (http://www.affymetrix.com). Annotations and expression intensities for the probe sets are presented in Supplementary Table 1. Note that *MLH1* expression was specifically suppressed in the MSI$^+$ samples. **(b)** Samples were projected into a virtual space with coordinates calculated by correspondence analysis of the 24 probe sets shown in **(a)**. Correspondence analysis was performed with ViSta software (http://www.visualstats.org) for all genes showing a significant difference.

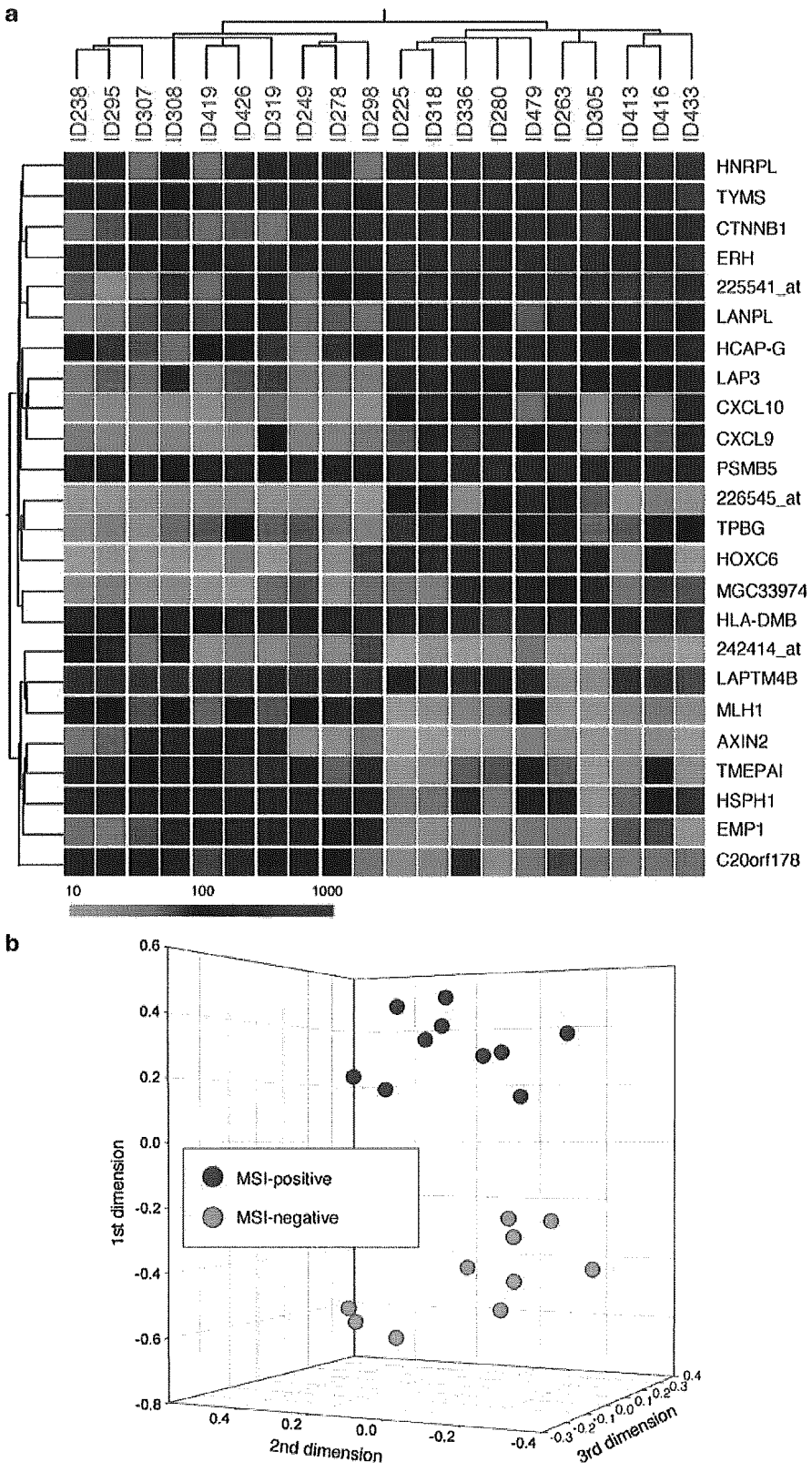
a
ID238
ID295
ID307
ID308
ID419
ID426
ID319
ID249
ID278
ID298
ID225
ID318
ID336
ID280
ID479
ID263
ID305
ID413
ID416
ID433
HNRPL
TYMS
CTNNB1
ERH
225541_at
LANPL
HCAP-G
LAP3
CXCL10
CXCL9
PSMB5
226545_at
TPBG
HOXC6
MGC33974
HLA-DMB
242414_at
LAPTM4B
MLH1
AXIN2
TMEPAI
HSPH1
EMP1
C20orf178
10
100
1000
b
MSI-positive
MSI-negative
1st dimension
2nd dimension
3rd dimension

The isolated MSI-associated genes include *AXIN2* and *CTNNB1* (β-catenin), both of which encode key participants in the WNT signaling pathway (Tolwinski and Wieschaus, 2004). Dysregulation of ubiquitin-dependent degradation of β-catenin contributes to carcinogenesis in a variety of CRCs and hepatocellular carcinomas (Narayan and Roy, 2003). AXIN2, similar to AXIN1, functions as a scaffold protein to facilitate this ubiquitination process by recruiting adenomatous polyposis coli (APC), glycogen synthase kinase-3β, and β-catenin (Behrens *et al.*, 1998). Defects in the degradation of β-catenin have been shown to result from mutations in *AXIN1*, *AXIN2*, *APC*, or *CTNNB1* (Rubinfeld *et al.*, 1997; Liu *et al.*, 2000; Satoh *et al.*, 2000; Smith *et al.*, 2002). Our data therefore suggest that transcriptional suppression of *AXIN2* might represent a novel mechanism by which the function of the APC-AXIN–β-catenin complex is impaired in CRC.

To confirm the MSI-associated change in *AXIN2* expression, we measured the abundance of the corresponding mRNA in the original 20 study specimens by quantitative reverse transcription–polymerase chain reaction (RT–PCR) analysis (Figure 2a). Comparison of the amount of *AXIN2* mRNA determined by RT–PCR with that determined by microarray analysis yielded a Pearson's correlation coefficient (r) of 0.89, indicating that the two data sets were highly correlated ($P<0.001$). (Also see Supplementary Figure 1 for verification of microarray data by RT–PCR.)

With the use of RT–PCR, we then measured the amount of *AXIN2* mRNA in a larger number of samples (seven additional specimens of MSI$^+$ CRC, for a total of 17; 10 additional specimens of MSI$^-$ CRC, for a total of 20; three MSI$^+$ CRC cell lines; two MSI$^-$ CRC cell lines). The abundance of *AXIN2* transcripts in most of the MSI$^+$ CRC specimens and cell lines was reduced compared with that in the MSI$^-$ ones (Figure 2b); an *AXIN2*/*ACTB* transcript ratio of $<5\times10^{-4}$ was apparent in 13 of the 17 MSI$^+$ CRC specimens, but in only five of the 20 MSI$^-$ ones (Fisher's exact probability test, $P=0.003$). Importantly, a similar MSI-dependent suppression of *AXIN1* expression was not observed among these specimens ($P=0.31$) (data not shown).

Human *AXIN2* possesses a relatively large CpG island within its promoter region (nucleotide positions, chr17: 60986365–60987824). We therefore examined the methylation status of the CpG sites within this region by nucleotide sequencing after sodium bisulfite treatment. Extensive methylation of the CpG island in the *AXIN2* promoter was apparent in CRC specimens positive for MSI and for the loss of *AXIN2* expression (Figure 2c). The promoter region in the MSI$^+$ CRC cell line HCT116 (Wheeler *et al.*, 1999) was also heavily methylated. The *MLH1* promoter in HCT116 cells is not methylated, but the coding sequence of the gene contains a mutation that results in MSI (Wheeler *et al.*, 1999).

On the basis of these findings, we examined the methylation status of the *AXIN2* promoter in 37 clinical specimens and five cell lines by combined bisulfite restriction analysis (COBRA) (Xiong and Laird, 1997). CpG methylation was detected in five of the 17 MSI$^+$ specimens, but in none of the 20 MSI$^-$ specimens (Table 1; see Supplementary Table 2). Methylation of the *AXIN2* promoter was not detected in normal colon tissue obtained from the individuals with MSI$^+$ CRC (data not shown), suggesting that *AXIN2* methylation was a somatic event in these patients.

We then tested whether the amount of the encoded protein correlated with that of *AXIN2* mRNA in CRC specimens (Figure 2d). Immunohistochemical staining showed that AXIN2 was abundant in a specimen with a high mRNA content (ID308), but was present in much smaller amounts in two specimens with a low mRNA content (ID263, ID295). Although a large amount of *AXIN2* mRNA was not always associated with a large amount of protein, a small amount of mRNA was consistently associated with a small amount of protein (data not shown).

To examine directly whether epigenetic silencing of *AXIN2* is relevant to the change in the growth properties of CRC cells, we restored *AXIN2* expression, either by 5′-azacytidine treatment or by introduction of *AXIN2* cDNA, in an MSI$^+$ CRC cell line. 5′-Azacytidine inhibits *de novo* methylation of genomic DNA and thereby induces demethylation of the genome of proliferating cells (Christman, 2002). HCT116 cells were incubated for 3 days with various concentrations of 5′-azacytidine and were then subjected to COBRA for determination of the methylation status of the *AXIN2* promoter. Treatment with 5′-azacytidine reduced the level of methylation of the *AXIN2* promoter in a concentration-dependent manner (Figure 3a). This effect of 5′-azacytidine was accompanied by an increase in the amount of *AXIN2* mRNA in the cells (Figure 3b) as well as by the induction of cell death (Figure 3c).

Given that 5′-azacytidine likely affects the transcription of other genes in addition to that of *AXIN2*, the growth inhibitory effect observed in HCT116 cells might not have been attributable solely to the induction of *AXIN2* expression. To examine the direct effect of *AXIN2*, we introduced its cDNA into HCT116 cells by transfection. However, an introduction of *AXIN2* cDNA (even with the use of an inducible system) resulted in rapid cell death, and we could not establish stable transformants of cell lines with such expression constructs (data not shown). Therefore, we generated an amphotropic recombinant retrovirus that confers simultaneous expression of both an MYC epitope-tagged form of AXIN2 and mouse CD8. Human kidney 293 cells infected with this virus, but not those infected with a mock virus, expressed AXIN2 (Figure 3d). HCT116 cells were then infected with the virus and were subjected to affinity chromatography 48 h thereafter to isolate cells that express CD8. Given that CD8-expressing cells would be expected also to express AXIN2, this column purification step should result in rapid enrichment of AXIN2-expressing cells. The isolated cells indeed contained a substantial amount of *AXIN2* mRNA as revealed by RT–PCR (Figure 3e). The purified CD8$^+$ HCT116 cells were then cultured for 3 days to characterize their growth properties. Forced expression of AXIN2 resulted in marked inhibition of cell growth

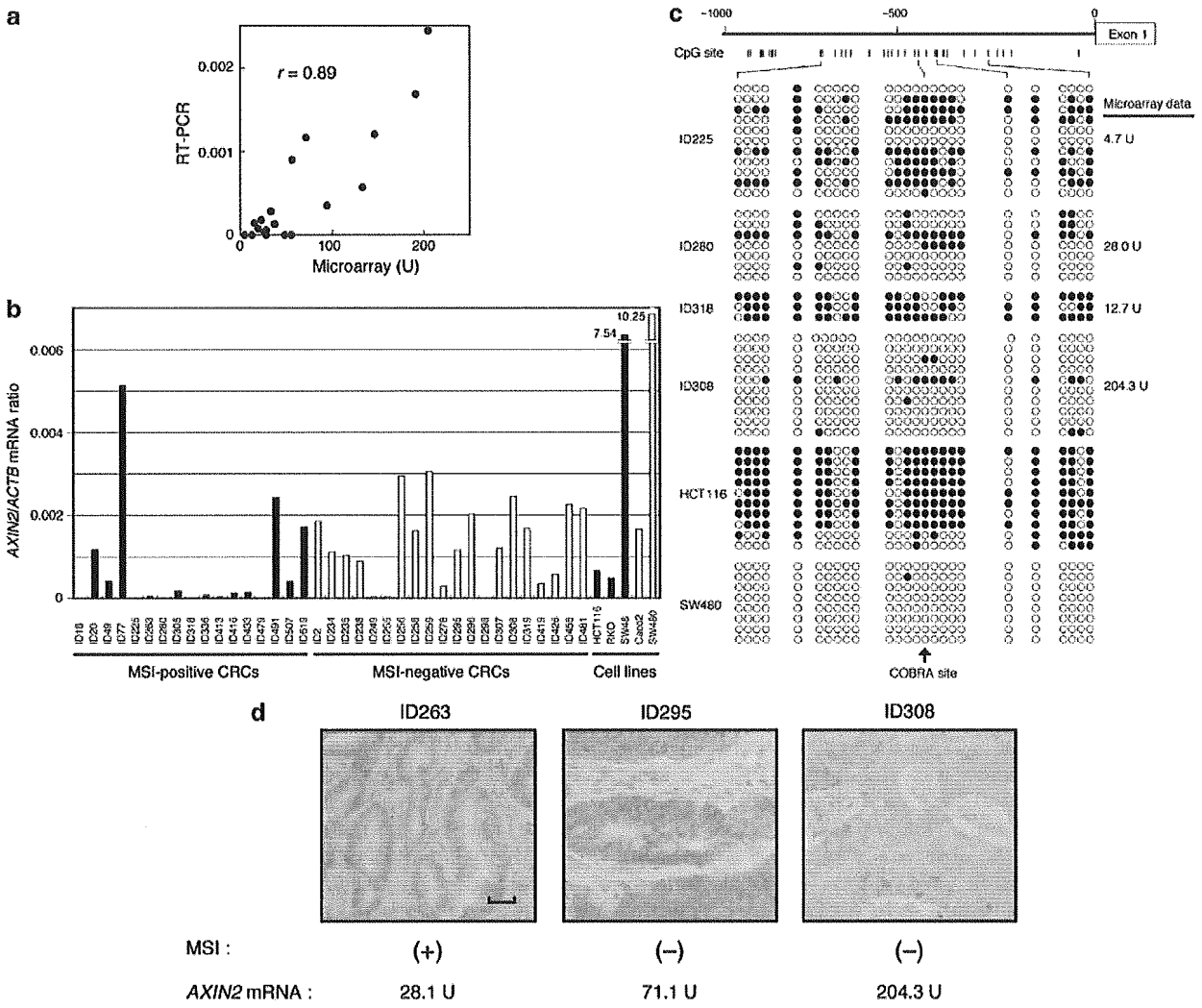

Figure 2 Suppression of *AXIN2* expression in CRCs positive for MSI. (**a**) Comparison of the abundance of *AXIN2* mRNA in study specimens as determined by microarray and RT–PCR analyses. For the latter, the amount of *AXIN2* mRNA was expressed relative to that of *ACTB* mRNA. Pearson's correlation coefficient (*r*) for the comparison is indicated. Portions of double-stranded cDNA were subjected to PCR with a QuantiTect SYBR Green PCR Kit (Qiagen). The amplification protocol comprised incubations at 94°C for 15 s, 63°C for 30 s, and 72°C for 60 s. Incorporation of the SYBR Green dye into PCR products was monitored in real time with an ABI PRISM 7700 sequence detection system (PE Applied Biosystems), thereby allowing determination of the threshold cycle (C_T) at which exponential amplification of products begins. The amount of target cDNAs relative to that of the β-actin (*ACTB*) cDNA was calculated from the C_T values with the use of Sequence Detector ver. 1.6.3 software (PE Applied Biosystems). The primers used for PCR amplification were 5′-CTGGCTCCAGAAGATCACAAAG-3′ and 5′-ATCTCCTCAAACACCGCTCCA-3′ for *AXIN2* and 5′-CCATCATGAAGTGTGACGTGG-3′ and 5′-GTCCGCCTAGAAGCATTTGCG-3′ for *ACTB*. (**b**) Comparison of the amount of *AXIN2* mRNA relative to that of *ACTB* mRNA (as determined by RT–PCR) between MSI^+ (closed bars) and MSI^- (open bars) CRC specimens and cell lines. (**c**) Genomic DNA of the indicated clinical specimens and CRC cell lines was treated with sodium bisulfite (Koinuma *et al*., 2004), after which the *AXIN2* promoter region was amplified by PCR with the primers 5′-TTGTATATAGTTTA GYGGTTGGG-3′ and 5′-AAATCTAAACTCCCTACACACTT-3′. Closed and open circles indicate methylated and unmethylated CpG sites, respectively. The positions of the CpG sites are indicated at the top, the *Hha*I digestion site for COBRA is indicated by the arrow, and the microarray data for *AXIN2* expression are shown on the right. (**d**) Immunohistochemical analysis of the indicated clinical specimens with antibodies to AXIN2. The MSI status and the expression level of *AXIN2* determined by microarray analysis are indicated. Immunohistochemical analysis of AXIN2 expression was performed as described previously (Leung *et al*., 2002). Sections (5 μm) of formalin-fixed, paraffin-embedded tissue were mounted on Probe-On slides (Fisher Scientific), which were then incubated first for 1 h at room temperature with 1.5% normal horse serum and then overnight at 4°C with goat polyclonal antibodies to AXIN2 (Santa Cruz Biotechnology). Immune complexes were detected by the avidin–biotin–peroxidase method with 3,3′-diaminobenzidine as the chromogenic substrate (Vectastain ABC kit, Vector Laboratories). The sections were counterstained with hematoxylin. Scale bar, 50 μm.

(Figure 3f), indicating that silencing of *AXIN2* is indeed relevant to tumorigenesis. We also examined if the expression of *AXIN2* directly suppresses the WNT signaling pathway. For this purpose, we utilized a luciferase-based reporter plasmid (TOPflash) for the T-cell factor (TCF) activity, which is a direct target of

β-catenin (Korinek *et al.*, 1997). As shown in Figure 3g, a forced expression of *AXIN2* induced a marked suppression in the luciferase activity in HCT116 cells. On the other hand, *AXIN2* did not affect luciferase activity driven by a mutated, nonfunctional TCF-binding sites (FOPflash). These data clearly indicate that AXIN2 is involved in the WNT–APC–β-catenin pathway in CRCs.

We have demonstrated preferential transcriptional silencing of *AXIN2* in MSI$^+$ CRCs. Recently, mutations within exon 7 of the *AXIN2* gene have been reported in MSI$^+$ CRC specimens (Liu *et al.*, 2000; Wu *et al.*, 2001). We have thus analysed the nucleotide sequence of the *AXIN2* gene among our MSI$^+$ samples ($n=9$). Sequencing of the *AXIN2* exon 7 has revealed that only one patient (ID no. 263) carried a mutated *AXIN2* gene in one allele (data not shown). A deletion of a cytosine residue at the nucleotide position 2096 of the *AXIN2* cDNA (GenBank Accession Number, AF078165) led to a frame shift in the open-reading frame in this patient, introducing a premature termination codon in AXIN2 protein at the amino-acid position of 688. However, majority of the patients had intact *AXIN2* genes, indicating that silencing, but not mutation, of *AXIN2* is the main pathway to impede the *AXIN2* function.

The COBRA experiments revealed that the promoter region of *AXIN2* was extensively methylated in MSI$^+$ CRCs but not in MSI$^-$ CRCs. Although the difference in the frequency of *AXIN2* methylation between these two classes of tumor was significant (Fisher's exact probability test, $P=0.003$), the frequency for the MSI$^+$ specimens was still only 29% and therefore was not able to account for all the observed instances of suppression of *AXIN2* expression. We judged COBRA data as positive for methylation if $\geqslant 10\%$ of the PCR products were digested by *Hha*I. However, a small proportion ($<10\%$) of the PCR products was digested in the analysis of $\sim 50\%$ of MSI$^+$ CRC specimens (data not shown), indicating that alterations in the methylation status of the *AXIN2* promoter were more widespread. It is therefore possible that CpG sites other than that targeted by COBRA are more frequently methylated in MSI$^+$ CRCs and are more important for transcriptional regulation.

Similar promoter methylation has been recently described for other genes important for the WNT signaling pathway. The genes for secreted frizzled-related proteins are thus epigenetically silenced in MSI$^+$ CRCs, resulting in constitutive activation of the WNT pathway (Suzuki *et al.*, 2004). CpG sites within the *APC* promoter were also found to be frequently methylated in CRCs and other cancers (Esteller *et al.*, 2000; Zysman *et al.*, 2002). These data thus suggest that not only genetic mutations but also epigenetic silencing might play an important role in tumorigenesis mediated by activation of the WNT pathway.

Methylation of the *APC* promoter in endometrial cancer has been shown to occur preferentially in MSI$^+$ tumors (Zysman *et al.*, 2002). Despite the lack of an MSI-associated difference in the expression of *APC* in our CRC specimens (data not shown), the results of this previous study together with our present findings suggest the possibility that genes related to the WNT signaling pathway are targeted for methylation specifically in cancers with MSI. Our data further indicate that such methylation in MSI$^+$ cancers may be directly relevant to the mechanism of malignant transformation through epigenetic silencing of tumor suppressor genes. MSI$^+$ CRCs have been thought to arise through genetic events distinct from those that underlie MSI$^-$ cancers (Rajagopalan and Lengauer, 2004), which are frequently associated with aneuploidy and mutations in WNT pathway genes such as *APC* and *CTNNB1*. However, our data indicate that the molecular mechanisms for malignant transformation overlap between MSI$^+$ and MSI$^-$ CRCs.

Figure 3 Induction of cell death by restoration of *AXIN2* expression in a CRC cell line with a methylated *AXIN2* promoter. (**a**) HCT116 cells were incubated for 72 h with 0, 0.2, or 1 μM 5′-azacytidine and were then subjected to COBRA for determination of the methylation status of the *AXIN2* promoter (Xiong and Laird, 1997). Genomic DNA was denatured, incubated for 16 h at 55°C in 3.1 M sodium bisulfite, and then subjected to PCR with the primers in Figure 2c. The PCR products were then digested with the restriction endonuclease *Hha*I (Takara Bio), and the resulting DNA fragments were fractionated by polyacrylamide gel electrophoresis. The gel was stained with SYBR Green I (Takara Bio) and scanned with an LAS3000 imaging system (Fuji Film). Genomic fragments were determined to be positive for CpG methylation if $\geqslant 10\%$ of the PCR products were cleaved by the restriction endonuclease. Lane M, DNA size markers (50-bp ladder). (**b**) The cells from (**a**) were also subjected to RT–PCR analysis for determination of the amount of *AXIN2* mRNA relative to that of *ACTB* mRNA. (**c**) Cells treated as in (**a**) with 0, 0.2, 1, or 5 μM 5′-azacytidine were examined by light microscopy. Cell death was estimated by counting the remaining viable cells in each culture dish by the dye-exclusion method. Scale bar, 50 μm. (**d**) Human kidney 293 cells infected with either a mock virus or a recombinant virus encoding both MYC epitope-tagged AXIN2 and mouse CD8. A human cDNA for AXIN2 tagged at its NH_2-terminus with the MYC epitope sequence was ligated into the pMX-iresCD8 retroviral plasmid (Yamashita *et al.*, 2001) to yield pMX-AXIN2-MYC-iresCD8. The latter plasmid was introduced into BOSC23 cells together with pE-ampho and pGP packaging plasmids (Takara Bio) by transfection with the use of Lipofectamine (Invitrogen). The culture supernatant containing recombinant viruses was added to 293 cells with 4 μg/ml of polybrene (Sigma). Cells were then subjected to immunoprecipitation with the antibodies to MYC (9E10, Roche Diagnostics), and to immunoblot analysis with the same antibodies. (**e**) HCT116 cells infected with the viruses in (**d**) were subjected to affinity chromatography to isolate CD8$^+$ cells, which were then subjected to RT–PCR analysis for quantitation of *AXIN2* mRNA relative to the amount of *ACTB* mRNA. (**f**) The CD8$^+$ fractions in (**e**) were seeded at a density of 5×10^4 cells/dish and cultured for 72 h, after which the ratio of the final cell number to the initial value was determined. Data are means + s.d. of triplicate from a representative experiment. The *P*-value for the indicated comparison was determined by Student's *t* test. (**g**) HCT116 cells were seeded at a density of 2.5×10^6 cells/6 cm dish. After 24 h of incubation, the cells were transfected, with the use of Lipofectamine, with 2 μg of pMX-AXIN2-MYC-iresCD8 (AXIN2) or pMX-iresCD8 (Mock). For the reporter plasmids, 0.5 μg of pGL4 (Promega, Madison, WI, USA) plus either 0.5 μg of pTOPflash or 0.5 μg of pFOPflash (both from Upstate Biotechnology, Lake Placid, NY, USA) were added to the lipofection mix. The activity of *Photinus pyralis* luciferase was measured after 24 h of incubation with the use of the Dual-luciferase reporter assay system (Promega), and normalized on the basis of the activity of *Renilla reniformis* luciferase produced by pGL4. Data are shown as the mean value + s.d. of triplicate samples.

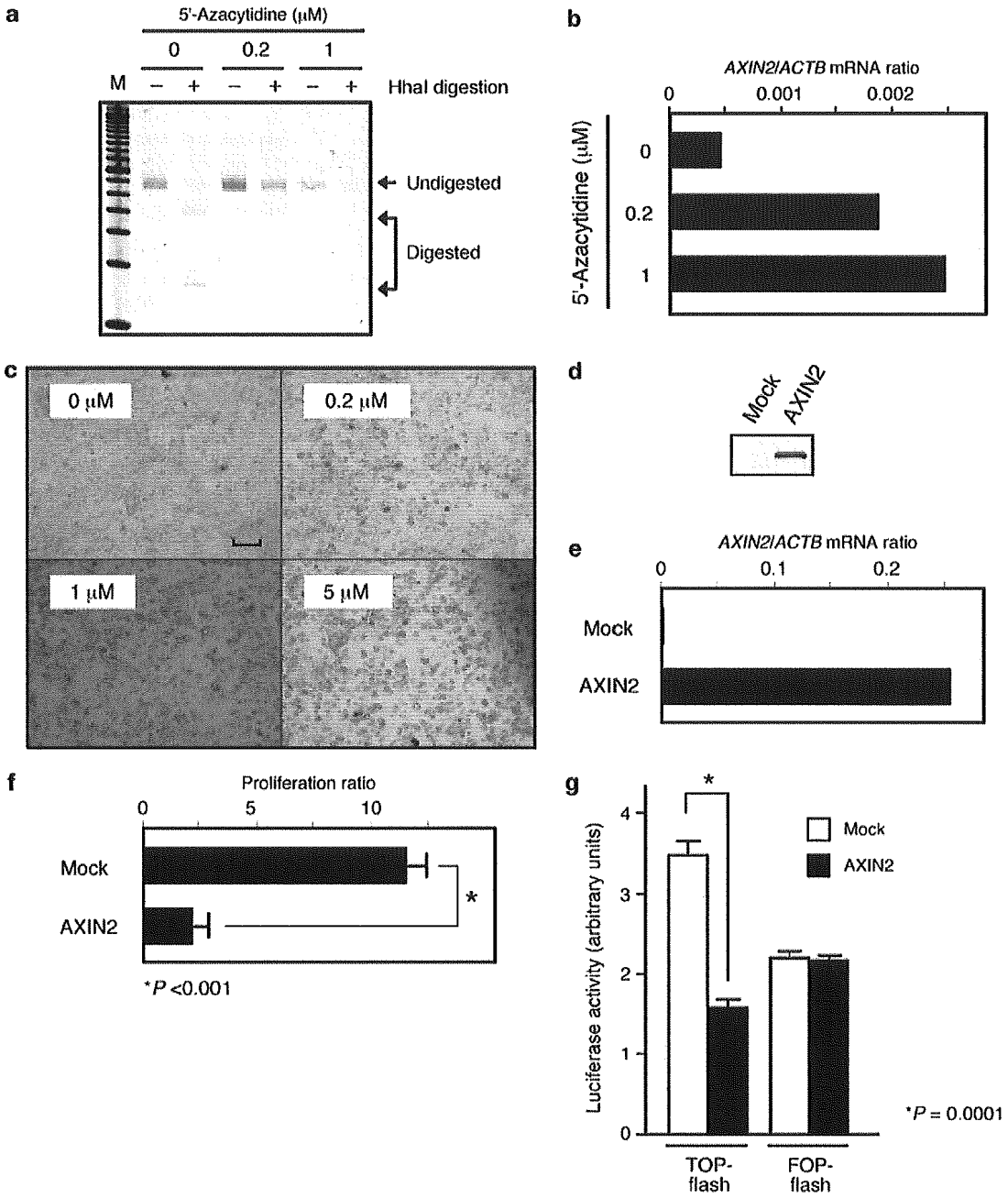

Acknowledgements

We thank M Toyota and SN Thibodeau for critical reading of the manuscript and helpful suggestions. This study was supported in part by a grant for Third-Term Comprehensive Control Research for Cancer from the Ministry of Health, Labor, and Welfare of Japan, and by a grant for 'High-Tech Research Center' Project for Private Universities: Matching Fund Subsidy (2002–2006) from the Ministry of Education, Culture, Sports, Science, and Technology of Japan.

References

Alon U, Barkai N, Notterman DA, Gish K, Ybarra S, Mack D *et al.* (1999). *Proc Natl Acad Sci USA* **96**: 6745–6750.

Behrens J, Jerchow BA, Wurtele M, Grimm J, Asbrand C, Wirtz R *et al.* (1998). *Science* **280**: 596–599.

Boland CR, Thibodeau SN, Hamilton SR, Sidransky D, Eshleman JR, Burt RW *et al.* (1998). *Cancer Res* **58**: 5248–5257.

Bronner CE, Baker SM, Morrison PT, Warren G, Smith LG, Lescoe MK *et al.* (1994). *Nature* **368**: 258–261.

Christman JK. (2002). *Oncogene* **21**: 5483–5495.
Cunningham JM, Christensen ER, Tester DJ, Kim CY, Roche PC, Burgart LJ *et al.* (1998). *Cancer Res* **58**: 3455–3460.
Esteller M, Sparks A, Toyota M, Sanchez-Cespedes M, Capella G, Peinado MA *et al.* (2000). *Cancer Res* **60**: 4366–4371.
Fellenberg K, Hauser NC, Brors B, Neutzner A, Hoheisel JD, Vingron M. (2001). *Proc Natl Acad Sci USA* **98**: 10781–10786.
Fishel R, Lescoe MK, Rao MR, Copeland NG, Jenkins NA, Garber J *et al.* (1993). *Cell* **75**: 1027–1038.
Ionov Y, Peinado MA, Malkhosyan S, Shibata D, Perucho M. (1993). *Nature* **363**: 558–561.
Issa JP. (2004). *Nat Rev Cancer* **4**: 988–993.
Kinzler KW, Vogelstein B. (1996). *Cell* **87**: 159–170.
Koinuma K, Shitoh K, Miyakura Y, Furukawa T, Yamashita Y, Ota J *et al.* (2004). *Int J Cancer* **108**: 237–242.
Korinek V, Barker N, Morin PJ, van Wichen D, de Weger R, Kinzler KW *et al.* (1997). *Science* **275**: 1784–1787.
Lengauer C, Kinzler KW, Vogelstein B. (1998). *Nature* **396**: 643–649.
Leung JY, Kolligs FT, Wu R, Zhai Y, Kuick R, Hanash S *et al.* (2002). *J Biol Chem* **277**: 21657–21665.
Liu W, Dong X, Mai M, Seelan RS, Taniguchi K, Krishnadath KK *et al.* (2000). *Nat Genet* **26**: 146–147.
Miyakura Y, Sugano K, Konishi F, Ichikawa A, Maekawa M, Shitoh K *et al.* (2001). *Gastroenterology* **121**: 1300–1309.
Narayan S, Roy D. (2003). *Mol Cancer* **2**: 41.
Ohki-Kaneda R, Ohashi J, Yamamoto K, Ueno S, Ota J, Choi YL *et al.* (2004). *Biochem Biophys Res Commun* **320**: 1328–1336.
Papadopoulos N, Nicolaides NC, Wei YF, Ruben SM, Carter KC, Rosen CA *et al.* (1994). *Science* **263**: 1625–1629.
Rajagopalan H, Lengauer C. (2004). *Nature* **432**: 338–341.
Rubinfeld B, Robbins P, El-Gamil M, Albert I, Porfiri E, Polakis P. (1997). *Science* **275**: 1790–1792.
Satoh S, Daigo Y, Furukawa Y, Kato T, Miwa N, Nishiwaki T *et al.* (2000). *Nat Genet* **24**: 245–250.
Smith G, Carey FA, Beattie J, Wilkie MJ, Lightfoot TJ, Coxhead J *et al.* (2002). *Proc Natl Acad Sci USA* **99**: 9433–9438.
Suzuki H, Watkins DN, Jair KW, Schuebel KE, Markowitz SD, Dong Chen W *et al.* (2004). *Nat Genet* **36**: 417–422.
Tolwinski NS, Wieschaus E. (2004). *Trends Genet* **20**: 177–181.
Toyota M, Ahuja N, Ohe-Toyota M, Herman JG, Baylin SB, Issa JP. (1999). *Proc Natl Acad Sci USA* **96**: 8681–8686.
Veigl ML, Kasturi L, Olechnowicz J, Ma AH, Lutterbaugh JD, Periyasamy S *et al.* (1998). *Proc Natl Acad Sci U S A* **95**: 8698–8702.
Wheeler JM, Beck NE, Kim HC, Tomlinson IP, Mortensen NJ, Bodmer WF. (1999). *Proc Natl Acad Sci USA* **96**: 10296–10301.
Wu R, Zhai Y, Fearon ER, Cho KR. (2001). *Cancer Res* **61**: 8247–8255.
Xiong Z, Laird PW. (1997). *Nucleic Acids Res* **25**: 2532–2534.
Yamashita Y, Kajigaya S, Yoshida K, Ueno S, Ota J, Ohmine K *et al.* (2001). *J Biol Chem* **276**: 39012–39020.
Zysman M, Saka A, Millar A, Knight J, Chapman W, Bapat B. (2002). *Cancer Res* **62**: 3663–3666.

Supplementary Information accompanies the paper on Oncogene website (http://www.nature.com/onc).

Available online at www.sciencedirect.com
SCIENCE DIRECT®
Leukemia Research 29 (2005) 943–949
Leukemia Research
www.elsevier.com/locate/leukres

Retroviral expression screening of oncogenes in natural killer cell leukemia

Young Lim Choi [a, b], Ryozo Moriuchi [c], Mitsujiro Osawa [d], Atsushi Iwama [d], Hideki Makishima [e], Tomoaki Wada [a], Hiroyuki Kisanuki [a], Ruri Kaneda [a], Jun Ota [a, f], Koji Koinuma [a], Madoka Ishikawa [a], Shuji Takada [a], Yoshihiro Yamashita [a], Kazuo Oshimi [b], Hiroyuki Mano [a, f, *]

[a] *Division of Functional Genomics, Jichi Medical School, 3311-1 Yakushiji, Kawachigun, Tochigi 329-0498, Japan*
[b] *Division of Hematology, Department of Medicine, Juntendo University School of Medicine, Tokyo, Japan*
[c] *Department of Molecular Microbiology and Immunology, Nagasaki University Graduate School of Medicine, Nagasaki, Japan*
[d] *Center for Experimental Medicine, Institute of Medical Science, University of Tokyo, Tokyo, Japan*
[e] *Second Department of Internal Medicine, Shinshu University School of Medicine, Nagano, Japan*
[f] *CREST, Japan Science and Technology Agency, Saitama, Japan*

Received 17 October 2004; accepted 22 January 2005
Available online 24 February 2005

Abstract

Aggressive natural killer cell leukemia (ANKL) is an intractable malignancy that is characterized by the outgrowth of NK cells. To identify transforming genes in ANKL, we constructed a retroviral cDNA expression library from an ANKL cell line KHYG-1. Infection of 3T3 cells with recombinant retroviruses yielded 33 transformed foci. Nucleotide sequencing of the DNA inserts recovered from these foci revealed that 31 of them encoded KRAS2 with a glycine-to-alanine mutation at codon 12. Mutation-specific PCR analysis indicated that the *KRAS* mutation was present only in KHYG-1 cells, not in another ANKL cell line or in clinical specimens ($n = 8$).

Keywords: Aggressive NK cell leukemia; cDNA expression library; Retrovirus; KRAS2 oncogene

1. Introduction

Outgrowth of $CD3^{-}CD16/CD56^{+}$ natural killer (NK) cells in peripheral blood is diagnosed as either chronic NK lymphocytosis (CNKL) or aggressive NK cell leukemia (ANKL) [1,2]. Whereas the former condition has an indolent clinical course with few symptoms, the latter is characterized by chemoresistance and multiorgan failure and has a poor outcome.

The Epstein–Barr virus (EBV) genome is frequently present episomally in ANKL cells [3], suggesting a role for EBV in disease pathogenesis. However, little is known of how infection with EBV might trigger clonal growth of NK cells. Inactivation of tumor suppressor genes has been associated with NK cell neoplasia. For instance, a homozygous deletion of the genes for p16INK4A, p15INK4B, or p14ARF has been detected [4]. Additionally, inactivating mutations of the FAS gene have been found in nasal NK/T cell lymphoma [5].

A few studies have identified a potential contribution of oncogenes to NK cell malignancy. Mutations that affect codons 13 or 22 of *KRAS2* were found in NK/T cell lymphoma [6] but not in ANKL [7]. Furthermore, although mutations in *KIT* were associated with NK/T cell lymphoma, transforming activity of the mutant KIT proteins was not demonstrated [8]. A role for oncogenes in ANKL has not been identified to date.

Functional screening based on transforming ability is one potential approach to the efficient isolation of tumor-promoting genes in ANKL. Focus formation assays with

* Corresponding author. Tel.: +81 285 58 7449; fax: +81 285 44 7322.
E-mail address: hmano@jichi.ac.jp (H. Mano).

0145-2126/$ – see front matter © 2005 Elsevier Ltd. All rights reserved.
doi:10.1016/j.leukres.2005.02.002

mouse 3T3 fibroblasts have indeed proved successful for the identification of oncogenes in human cancer [9]. In such screening assays, genomic DNA isolated from cancer specimens is used to transfect 3T3 cells and the formation of transformed cell foci is then evaluated. Expression of the exogenous genes in such experiments is driven by their own promoters or enhancers, however, so that oncogenes can exert transforming effects in 3T3 cells only if their regulatory regions are active in fibroblasts. Given the distinct developmental origins of NK cells and fibroblasts, expression of oncogenes associated with ANKL in 3T3 cells under these conditions is not guaranteed.

This problem might be expected to be overcome by the expression of test cDNAs under the control of an ectopic promoter in 3T3 cells. We have therefore constructed a retroviral cDNA expression library from the ANKL cell line KHYG-1 [10] and used this library to infect 3T3 cells. In preparation of the cDNA library, we took advantage of a polymerase chain reaction (PCR)-based system that preferentially amplifies full-length cDNAs. The resulting library was found to have sufficient complexity and to contain a high percentage of full-length cDNAs. Focus formation assays with 3T3 cells resulted in the identification of *KRAS2* as a transforming gene in KHYG-1 cells.

2. Materials and methods

2.1. Cell culture and clinical samples

KHYG-1 and NKL cells [11] were kindly provided by M. Yagita and Y. Yokota, respectively, and were cultured in RPMI 1640 medium (Invitrogen, Carlsbad, CA) supplemented with 10% fetal bovine serum (Invitrogen) and human interleukin-2 (20 U/mL) (Roche, St. Louis, MO). The BOSC23 packaging cell line for ecotropic retroviruses [12] and mouse 3T3 fibroblasts were maintained in Dulbecco's modified Eagle's medium (DMEM)–F12 (Invitrogen) supplemented with 10% fetal bovine serum and 2 mM L-glutamine.

Mononulear cells were isolated by Ficoll–Hypaque density gradient centrifugation from peripheral blood of the subjects with informed consent. The cells were incubated with anti-CD3 MicroBeads (Miltenyi Biotec, Auburn, CA), and loaded onto MIDI-MACS magnetic cell separation columns (Miltenyi Biotec) to remove $CD3^+$ cells. The flow-through was then mixed with anti-CD56 MicroBeads (Miltenyi Biotec), and was subjected to a MINI-MACS column for the "positive selection" of $CD56^+$ cells. Cells bound specifically to the column was then eluted according to the manufacturer's instructions.

2.2. Construction of a retrovirus library

Total RNA was extracted from KHYG-1 cells with the use of an RNeasy Mini column and RNase-free DNase (Qiagen, Valencia, CA), and first-strand cDNA was synthesized from the RNA with PowerScript reverse transcriptase, a SMART IIA oligonucleotide, and CDS primer IIA (Clontech, Palo Alto, CA). The resulting cDNA molecules were then amplified for 12 cycles with 5′-PCR primer IIA and a SMART PCR cDNA synthesis kit (Clontech), with the exception that LA Taq polymerase (Takara Bio, Shiga, Japan) was substituted for the Advantage 2 DNA polymerase provided with the kit. The PCR products were treated with proteinase K, rendered blunt-ended with T4 DNA polymerase, and ligated to a *Bst*XI adapter (Invitrogen). Unbound adapters were removed with a cDNA size fractionation column (Invitrogen), and the modified cDNAs were ligated into the pMX retroviral plasmid (kindly provided by T. Kitamura) [13] that had been digested with *Bst*XI. The pMX-cDNA plasmids were introduced into ElecroMax DH10B cells (Invitrogen) by electroporation.

2.3. Focus formation assay

BOSC23 cells (1.8×10^6) were seeded onto 6-cm culture plates, cultured for 1 day, and then transfected with a mixture comprising 2 μg of retroviral plasmids, 0.5 μg of pGP plasmid (Takara Bio), 0.5 μg of pE-eco plasmid (Takara Bio), and 18 μL of Lipofectamine reagent (Invitrogen). Two days after transfection, polybrene (Sigma, St. Louis, MO) was added at a concentration of 4 μg/mL to the culture supernatant, which was then used to infect 3T3 cells for 48 h. For the focus formation assay, the culture medium of 3T3 cells was changed to DMEM–high glucose (Invitrogen) supplemented with 5% calf serum and 2 mM L-glutamine. Transformed foci were isolated after 3 weeks of culture.

2.4. Recovery of cDNAs from 3T3 cells

Each 3T3 cell clone was harvested with a cloning syringe and cultured independently in a 10-cm culture plate. Genomic DNA was subsequently extracted from the cells and subjected to PCR with 5′-PCR primer IIA and LA Taq polymerase for 50 cycles of 98 °C for 20 s and 68 °C for 6 min. Amplified genomic fragments were purified by gel electrophoresis and ligated into the pT7Blue-2 vector (EMD Biosciences, San Diego, CA) for nucleotide sequencing.

2.5. Mutation-specific PCR for KRAS2

Detection of $KRAS2^{G12A}$ cDNA was performed as described previously [14] but with minor modifications. In brief, a 5′-region of *KRAS2* cDNA was amplified from oligo(dT)–primed cDNA by PCR with 5′-RAS primer (5′-ACTGAATATAAACTTGTGGTAGTTGGACCT-3′; the underlined cytosine was incorporated to generate a *Bst*NI site) and 3′-RAS primer A (5′-CTGTGTCGAGAATATCCAAGAGACA-3′). The PCR product was subjected to digestion with *Bst*NI (New England Biolabs, Beverly, MA) and then to a second PCR with 5′-RAS primer and 3′-RAS primer B (5′-CTGTGTCGAGAATCCAGGAGACA-3′; the under-

lined guanine was incorporated to generate a *Bst*NI site). The second PCR product was then also subjected to digestion with *Bst*NI, and the resulting DNA fragments were separated by agarose gel electrophoresis.

3. Results

3.1. Construction of a full-length cDNA expression library for KHYG-1 cells

Full-length cDNAs were selectively amplified from mRNA of KHYG-1 cells and ligated into the retroviral vector pMX. We obtained a total of 5.61×10^6 colony-forming units (cfu) of independent plasmid clones. To evaluate the quality of the library, we randomly selected 40 clones and examined the incorporated cDNAs. Thirty-nine of the 40 clones contained inserts with an average size of 2.03 kbp. The cDNA inserts from 20 out of these 39 clones were sequenced from both ends, and the determined sequences were used to screen, with the BLAT search program [15], the nucleotide sequence database assembled as of July 2003 by the Genome Bioinformatics Group of the University of California at Santa Cruz (http://genome.ucsc.edu/). Both ends of 14 of the 20 cDNAs could be matched to the mRNA sequences of known genes, and 13 of these cDNAs included complete open reading frames (data not shown). We therefore concluded that the retroviral cDNA expression library was of sufficient complexity and sufficiently enriched in full-length cDNAs for the present study.

3.2. Identification of $KRAS2^{G12A}$ in KHYG-1 cells

We generated a recombinant ecotropic retrovirus library by introducing 7.1×10^5 cfu of the generated plasmids into a packaging cell line. This library was then used to infect mouse 3T3 fibroblasts. After culture of the infected cells for 3 weeks, we detected 33 transformed foci (Fig. 1). Each focus was isolated, expanded independently, and subjected to extraction of genomic DNA for the recovery of retroviral inserts by PCR with the primer used originally to amplify the cDNAs during construction of the library. In most instances, a single major DNA fragment was recovered from each genome (Fig. 2A), suggestive of original infection of a single 3T3 cell with a single retrovirus.

The recovered cDNA fragments were sequenced from both ends for all 33 clones. Screening of the human genome sequence database with the insert sequences revealed that those from 31 of the 33 clones (#1–#29, #31, #33) matched, with >98% identity, the sequence of human *KRAS2* (GenBank accession number, NM_004985). The genome of 3T3 clone ID #30 yielded two PCR fragments (Fig. 2A); the larger (~1.4 kbp) and the smaller (~0.9 kbp) fragments were revealed to be derived from β-actin (*ACTB*; GenBank accession number, NM_001101) and profilin 1 (*PFN1*; GenBank accession number, NM_005022) genes, respectively. The final 3T3 clone (#32) yielded a major PCR fragment corresponding to the gene for isocitrate dehydrogenase 3 (NAD^+) β (*IDH3B*; GenBank accession number, NM_006899).

KRAS2 belongs to the *RAS* gene family and is involved in a wide variety of human cancers [16]. Given that point

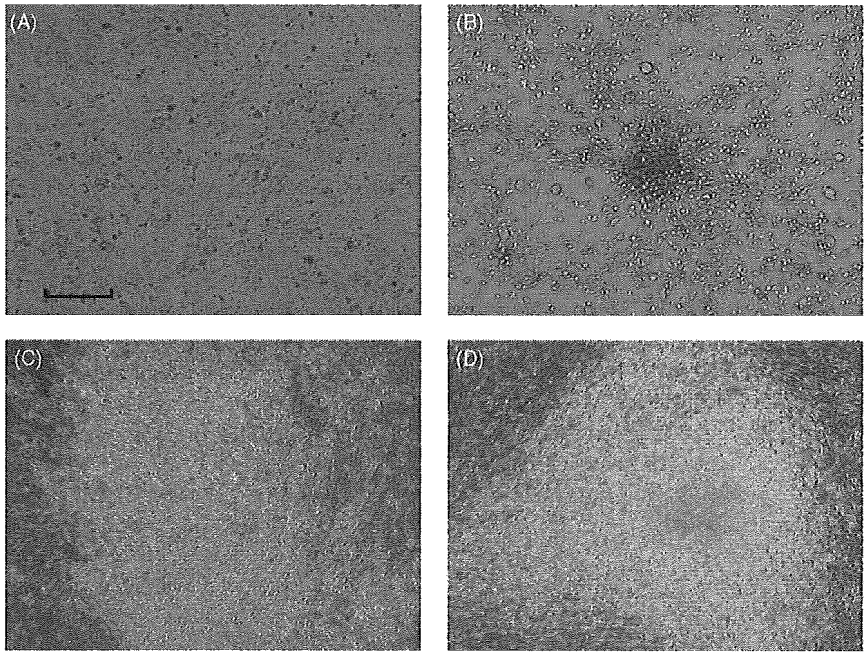

Fig. 1. Focus formation assay with a retroviral library derived from KHYG-1 cells. Mouse 3T3 cells were infected with the empty virus (A), a retrovirus expressing v-Ras as a positive control (B), or retroviruses from the KHYG-1 cell library (C and D). The cultures were photographed 3 weeks after infection. Scale bar, 100 μm.

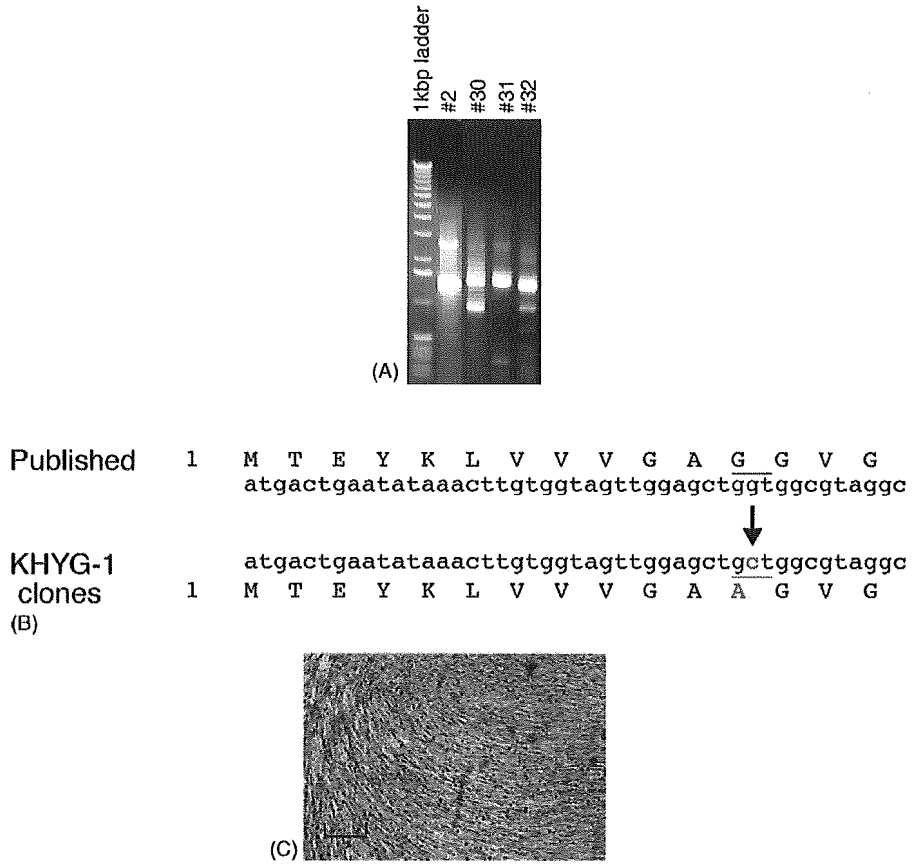

Fig. 2. Identification of a *KRAS* mutant gene with transforming activity: (A) Genomic DNA isolated from transformed 3T3 cell foci (clones #2, #30, #31, and #32) was subjected to PCR for amplification of the DNA inserts. The left lane contains DNA size markers (1-kbp DNA ladder; Invitrogen); (B) The nucleotide sequences of the DNA inserts derived from 31 of the 33 transformed foci matched that of *KRAS* with a single nucleotide substitution (G to C) in the second position of codon 12 that results in a change in the encoded amino acid from glycine to alanine; (C) A recombinant retrovirus encoding KRAS2^{G12A} was used to infect 3T3 cells. The cells were photographed after culture for 2 weeks. Scale bar, 50 μm.

mutations in *KRAS2* confer oncogenic activity, we compared the nucleotide sequences of the *KRAS2* cDNAs derived from KHYG-1 cells with the published sequence of the wild-type gene. Although oncogenic mutations have previously been shown to affect codons 12, 13, and 59 of *KRAS2*, all of the KHYG-1 cell cDNAs harbored the same mutation: the GGT sequence of codon 12 was changed to GCT, resulting in the substitution of an alanine residue for the glycine normally present at this position (Fig. 2B). To verify the transforming ability of *KRAS2*^{G12A}, we inserted the corresponding cDNA into the pMX retroviral vector and generated recombinant retroviruses for infection of 3T3 cells. The recipient 3T3 cells indeed underwent transformation (Fig. 2C), confirming that *KRAS2*^{G12A} possesses oncogenic activity.

3.3. Screening for *KRAS2*^{G12A} in NK cell leukemia

To determine whether *KRAS2*^{G12A} is frequently associated with NK cell leukemia, we applied a slightly modified version of a rapid screening method previously described by Kahn et al. [14]. *KRAS2* cDNA was first amplified by PCR with 5′-RAS primer and 3′-RAS primer A (Fig. 3A). The 3′ end of 5′-RAS primer corresponds to codon 11 of *KRAS2* but contains a cytosine substitution in the first position of codon 11, which generates a *Bst*NI recognition site [CC(T/A)GG] that includes the first and second positions of codon 12. The presence of a point mutation at the first or second position of codon 12 would therefore prevent digestion of the PCR product by *Bst*NI.

After *Bst*NI digestion, the PCR product was subjected to a second PCR with 5′-RAS primer and 3′-RAS primer B. Given that *Bst*NI digestion removes the binding site for 5′-RAS primer, only *KRAS2* cDNA with a mutation at the first or second position of codon 12 should yield a second PCR product. Even if *Bst*NI digestion of the initial PCR product was not complete and the second PCR amplified a trace amount of wild-type *KRAS2* cDNA, a second *Bst*NI digestion further discriminates between the wild-type and mutant genes. The 3′-RAS primer B thus contains a guanine substitution that generates a *Bst*NI site. The second PCR product of wild-type *KRAS2* cDNA would thus contain two *Bst*NI sites, whereas that of mutant *KRAS2* contains only one.

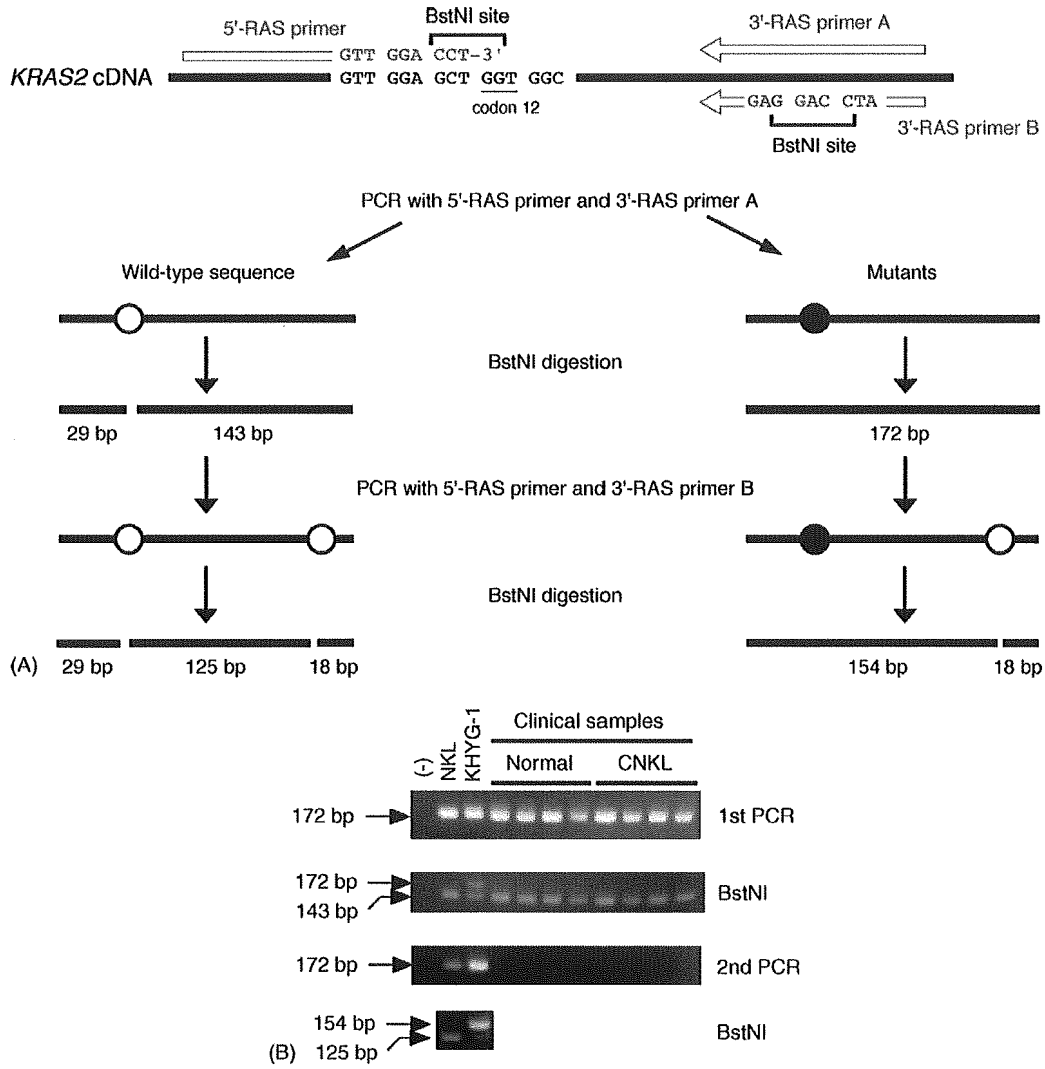

Fig. 3. Mutation-specific PCR analysis of NK cell leukemia cell lines and clinical specimens: (A) *KRAS2* cDNA was amplified with 5′-RAS primer and 3′-RAS primer A. The PCR product was subjected to digestion with *Bst*NI and then to a second PCR with 5′-RAS primer and 3′-RAS primer B. The second PCR product was also subjected to digestion with *Bst*NI. The nucleotides shown in red were incorporated into the primers to generate a *Bst*NI site. Open circles indicate *Bst*NI sites; closed circles indicate corresponding mutant sequences that are not susceptible to *Bst*NI; (B) cDNA isolated from the NKL and KHYG-1 cell lines as well as from $CD3^{-}CD56^{+}$ NK cell fractions derived from healthy volunteers (Normal) or individuals with CNKL was subjected to mutation-specific PCR analysis. A reaction without input DNA was also performed as a negative control (–). The size of DNA fragments is indicated on the left.

With this approach, we analyzed cDNA prepared from two ANKL cell lines (NKL and KHYG-1) and from $CD3^{-}CD56^{+}$ NK cell fractions purified from the peripheral blood of healthy individuals ($n=4$) and patients with CNKL ($n=4$). The first PCR step yielded a single DNA fragment of 172 bp from all samples. Furthermore, only the PCR product from KHYG-1 cells was refractory to *Bst*NI digestion, indicating that only KHYG-1 cells harbor a codon 12 mutation of *KRAS2*. The presence of the 143-bp band may indicate that KHYG-1 cells are heterozygous for the *KRAS2* mutation. The second PCR generated a 172-bp DNA fragment only with the NKL and KHYG-1 cell samples. Whereas this fragment derived from NKL cells was completely digested by *Bst*NI to generate a 125-bp band, *Bst*NI digestion of the fragment derived from KHYG-1 cells generated a band of 154 bp. Of all the samples analyzed, therefore, mutation of the first or second position of codon 12 of *KRAS2* was detected only in KHYG-1 cells.

4. Discussion

We have constructed a retroviral cDNA expression library for an ANKL cell line. Given that >97% (39/40) of the viral plasmids contained cDNA inserts and that the overall clone number was $>5 \times 10^6$, our library likely represents most of

the transcriptome of KHYG-1 cells. The high probability that the incorporated cDNAs are full length is also an important advantage for functional screening.

In our screening, most of the 3T3 transformants were found to have incorporated a single cDNA fragment corresponding to *KRAS2*^{G12A}, with only two transformants found to contain other cDNAs. One of these two cDNA inserts was derived from the gene for PFN1, a protein that binds to unpolymerized actin [17]. Homozygous deletion of *Pfn1* results in embryonic death in mice, with the encoded protein apparently being indispensable for cell growth or differentiation during embryonic development [18]. The other cDNA insert isolated from 3T3 transformants contained the entire open reading frame for IDH3B, which catalyzes the oxidative decarboxylation of isocitrate and is a key enzyme in the tricarboxylic acid cycle [19]. Neither *PFN1* nor *IDH3B* has previously been shown to possess oncogenic activity. It is currently under examination whether a long terminal repeat (LTR)-driven overexpression of *PFN1* or *IDH3B* leads focus formation in 3T3 cells.

Comparative genomic hybridization analysis identified a wide variety of genetic alterations at a high frequency in ANKL cells [20], suggesting that leukemogenesis in ANKL is associated with multiple steps of oncogene activation. An analysis of patients with NK cell neoplasia failed to detect any changes in the genes for members of the RAS and MYC families of proteins [7], however. This previous study did find a frequent increase in the abundance of the cell cycle regulator MDM2.

In contrast, we have detected a transforming *KRAS2* mutant gene in an ANKL cell line. Given that the mutation in codon 12 of this gene was detected by two different approaches (retroviral screening of PCR-amplified cDNAs and mutation-specific PCR), we conclude that it was not an artifact of PCR. KRAS2 is a GTP-binding protein with a relative molecular mass of ~21 kDa. Together with HRAS and NRAS, it plays an important role in cell growth and differentiation. Many mitogenic signals promote the loading of KRAS2 with GTP, which in turn triggers various downstream signaling events including activation of the mitogen-activated protein kinase (MAPK) pathway.

Activating mutations of *KRAS2* have been identified in a wide range of human cancers. Mutations of codon 12, for example, are associated with acute lymphoblastic leukemia [21], lung cancer [22], and pancreatic cancer [23]. No such mutations have previously been detected in association with ANKL, however. Although we have now identified a *KRAS2* mutation affecting codon 12 in the ANKL cell line KHYG-1, we did not detect this mutation in another ANKL cell line (NKL) or in $CD3^{-}CD56^{+}$ NK cell fractions isolated from healthy volunteers or from individuals with CNKL. Mutation of *KRAS2*, at least of codon 12 of this gene, might therefore be an infrequent event in NK cell neoplasia. Indeed, it remains possible that the detected *KRAS2* mutation is specific to the KHYG-1 cell line. Nevertheless, our identification of an activating *KRAS2* mutation in KHYG-1 cells might provide insight into the role of the RAS-MAPK signaling pathway in ANKL carcinogenesis. Furthermore, given the high quality of our retroviral expression library, the strategy adopted in the present study also might prove useful for the functional screening of genes associated with various clinical characteristics of ANKL, such as chemoresistance.

Acknowledgments

This work was supported in part by grants for Research on Human Genome and Tissue Engineering and for Third-Term Comprehensive Control Research for Cancer from the Ministry of Health, Labor, and Welfare of Japan, as well as by grants from Research Foundation for Community Medicine of Japan, Sankyo Foundation of Life Science, Takeda Science Foundation, and Mitsubishi Pharma Research Foundation. Y.-L.C conducted most of the experiments. R.M., M.O., A.I. and T.W. helped to establish a retroviral expression library. Hideki Makishima, J.O. and K.O. collected the ANKL specimens, and conducted the mutation-specific PCR method. H.K., R.K., K.K., M.I., S.T. and Y.Y. helped the 3T3 focus formation screening, and provided suggestions on molecular biology. Hiroyuki Mano designed this project with Y.-L.C., and was responsible for all aspects of this project.

References

[1] Harris NL, Jaffe ES, Diebold J, Flandrin G, Muller-Hermelink HK, Vardiman J, et al. World Health Organization classification of neoplastic diseases of the hematopoietic and lymphoid tissues: report of the Clinical Advisory Committee meeting, Airlie House, Virginia, November. J Clin Oncol 1999;17:3835–49.

[2] Oshimi K. Leukemia and lymphoma of natural killer lineage cells. Int J Hematol 2003;78:18–23.

[3] Gelb AB, van de Rijn M, Regula Jr DP, Cornbleet JP, Kamel OW, Horoupian DS, et al. Epstein–Barr virus-associated natural killer-large granular lymphocyte leukemia. Hum Pathol 1994;25:953–60.

[4] Sakajiri S, Kawamata N, Egashira M, Mori K, Oshimi K. Molecular analysis of tumor suppressor genes, Rb, p53, p16INK4A, p15INK4B and p14ARF in natural killer cell neoplasms. Jpn J Cancer Res 2001;92:1048–56.

[5] Takakuwa T, Dong Z, Nakatsuka S, Kojya S, Harabuchi Y, Yang WI, et al. Frequent mutations of Fas gene in nasal NK/T cell lymphoma. Oncogene 2002;21:4702–5.

[6] Hoshida Y, Hongyo T, Nakatsuka S, Nishiu M, Takakuwa T, Tomita Y, et al. Gene mutations in lymphoproliferative disorders of T and NK/T cell phenotypes developing in renal transplant patients. Lab Invest 2002;82:257–64.

[7] Sugimoto KJ, Kawamata N, Sakajiri S, Oshimi K. Molecular analysis of oncogenes, ras family genes (N-ras, K-ras, H-ras), myc family genes (c-myc, N-myc) and mdm2 in natural killer cell neoplasms. Jpn J Cancer Res 2002;93:1270–7.

[8] Hongyo T, Li T, Syaifudin M, Baskar R, Ikeda H, Kanakura Y, et al. Specific c-kit mutations in sinonasal natural killer/T-cell lymphoma in China and Japan. Cancer Res 2000;60:2345–7.

[9] Aaronson SA. Growth factors and cancer. Science 1991;254:1146–53.

[10] Yagita M, Huang CL, Umehara H, Matsuo Y, Tabata R, Miyake M, et al. A novel natural killer cell line (KHYG-1) from a patient with aggressive natural killer cell leukemia carrying a p53 point mutation. Leukemia 2000;14:922–30.
[11] Robertson MJ, Cochran KJ, Cameron C, Le JM, Tantravahi R, Ritz J, et al. Characterization of a cell line, NKL, derived from an aggressive human natural killer cell leukemia. Exp Hematol 1996;24:406–15.
[12] Pear WS, Nolan GP, Scott ML, Baltimore D. Production of high-titer helper-free retroviruses by transient transfection. Proc Natl Acad Sci USA 1993;90:8392–6.
[13] Onishi M, Kinoshita S, Morikawa Y, Shibuya A, Phillips J, Lanier LL, et al. Applications of retrovirus-mediated expression cloning. Exp Hematol 1996;24:324–9.
[14] Kahn SM, Jiang W, Culbertson TA, Weinstein IB, Williams GM, Tomita N, et al. Rapid and sensitive nonradioactive detection of mutant K-ras genes via 'enriched' PCR amplification. Oncogene 1991;6:1079–83.
[15] Kent WJ. BLAT—the BLAST-like alignment tool. Genome Res 2002;12:656–64.
[16] Ayllon V, Rebollo A. Ras-induced cellular events. Mol Membr Biol 2000;17:65–73.
[17] Goldschmidt-Clermont PJ, Janmey PA, Profilin. A weak CAP for actin and RAS. Cell 1991;66:419–21.
[18] Witke W, Sutherland JD, Sharpe A, Arai M, Kwiatkowski DJ. Profilin I is essential for cell survival and cell division in early mouse development. Proc Natl Acad Sci USA 2001;98:3832–6.
[19] Kim YO, Park SH, Kang YJ, Koh HJ, Kim SH, Park SY, et al. Assignment of mitochondrial NAD(+)-specific isocitrate dehydrogenase beta subunit gene (IDH3B) to human chromosome band 20p13 by in situ hybridization and radiation hybrid mapping. Cytogenet Cell Genet 1999;86:240–1.
[20] Siu LL, Wong KF, Chan JK, Kwong YL. Comparative genomic hybridization analysis of natural killer cell lymphoma/leukaemia. Recognition of consistent patterns of genetic alterations. Am J Pathol 1999;155:1419–25.
[21] Perentesis JP, Bhatia S, Boyle E, Shao Y, Shu XO, Steinbuch M, et al. RAS oncogene mutations and outcome of therapy for childhood acute lymphoblastic leukemia. Leukemia 2004;18:685–92.
[22] Santos E, Martin-Zanca D, Reddy EP, Pierotti MA, Della Porta G, Barbacid M. Malignant activation of a K-ras oncogene in lung carcinoma but not in normal tissue of the same patient. Science 1984;223:661–4.
[23] Motojima K, Urano T, Nagata Y, Shiku H, Tsurifune T, Kanematsu T. Detection of point mutations in the Kirsten-ras oncogene provides evidence for the multicentricity of pancreatic carcinoma. Ann Surg 1993;217:138–43.

Available online at www.sciencedirect.com
SCIENCE DIRECT®
ELSEVIER
Biochemical and Biophysical Research Communications 338 (2005) 1256–1262
BBRC
www.elsevier.com/locate/ybbrc

Transforming activity of the lymphotoxin-β receptor revealed by expression screening

Shin-ichiro Fujiwara [a,b,c], Yoshihiro Yamashita [a], Young Lim Choi [a], Tomoaki Wada [a], Ruri Kaneda [a,d], Shuji Takada [a], Yukio Maruyama [c], Keiya Ozawa [b], Hiroyuki Mano [a,d,*]

[a] *Division of Functional Genomics, Jichi Medical School, Tochigi 329-0498, Japan*
[b] *Division of Hematology, Jichi Medical School, Tochigi 329-0498, Japan*
[c] *First Department of Internal Medicine, Fukushima Medical University, Fukushima 960-1295, Japan*
[d] *CREST, Japan Science and Technology Agency, Saitama 332-0012, Japan*

Received 13 October 2005
Available online 24 October 2005

Abstract

Pancreatic ductal carcinoma (PDC) remains one of the most intractable human malignancies. To obtain insight into the molecular pathogenesis of PDC, we constructed a retroviral cDNA expression library with total RNA isolated from the PDC cell line MiaPaCa-2. Screening of this library with the use of a focus formation assay with NIH 3T3 mouse fibroblasts resulted in the identification of 13 independent genes with transforming activity. One of the cDNAs thus identified encodes an NH_2-terminally truncated form of the lymphotoxin-β receptor (LTBR). The transforming activity of this short-type LTBR in 3T3 cells was confirmed by both an in vitro assay of cell growth in soft agar and an in vivo assay of tumorigenicity in nude mice. The full-length (wild-type) LTBR protein was also found to manifest similar transforming activity. These observations suggest that LTBR, which belongs to the tumor necrosis factor receptor superfamily of proteins, may contribute to human carcinogenesis.

Keywords: Lymphotoxin-β receptor; Pancreatic ductal carcinoma; Retrovirus; cDNA expression library; Oncogene

Pancreatic ductal carcinoma (PDC) originates from pancreatic ductal cells and remains one of the most intractable human malignancies [1,2]. Effective therapy for PDC is hampered by the absence of specific clinical symptoms. At the time of diagnosis, most affected individuals are no longer candidates for surgical resection, and, even in patients who do undergo such surgery, the 5-year survival rate is only 20–30% [2].

The molecular pathogenesis of PDC has been the subject of intensive investigation. The gene *KRAS2* is frequently mutated and activated in PDC cells [3], and various tumor suppressor genes, including those for p53, p16, and BRCA2, are inactivated [4]. Furthermore, genetic or epigenetic alterations of genes important in apoptosis or in tumor cell invasion or metastasis have been detected in PDC cells [5]. However, mutations in *KRAS2* have also been identified in pancreatic tissue affected by nonmalignant chronic pancreatitis [6], and genetic changes truly specific to PDC remain to be uncovered. Improvement in the prognosis of individuals with PDC will require identification of the genetic or epigenetic alterations responsible for the aggressive nature of this cancer.

The focus formation assay with 3T3 or RAT1 fibroblasts has been extensively used to screen for transforming genes in various carcinomas [7]. Given that the expression of exogenous genes in this assay is usually controlled by their own promoters or enhancers, however, oncogenes are able to exert their transforming effects in the recipient cells only if these regulatory regions are active in fibroblasts, which is not always the case. Regulation of the transcription of test cDNAs by a promoter known to function efficiently in fibroblasts would be expected to

* Corresponding author. Fax: +81 285 44 7322.
E-mail address: hmano@jichi.ac.jp (H. Mano).

0006-291X/$ - see front matter © 2005 Elsevier Inc. All rights reserved.
doi:10.1016/j.bbrc.2005.10.080

ensure sufficient expression of the encoded protein in the focus formation assay. We have therefore now constructed a retroviral cDNA expression library from a human PDC cell line, MiaPaCa-2, and tested this library in the focus formation assay with 3T3 cells. For library construction, we took advantage of a polymerase chain reaction (PCR) system that preferentially amplifies full-length cDNAs. The resulting library had sufficient complexity with a high percentage of full-length cDNAs. With this library, we have revealed that the lymphotoxin-β receptor (LTBR) gene possesses transforming activity.

Materials and methods

Cell lines and culture. MiaPaCa-2, NIH 3T3, and BOSC23 cell lines were obtained from American Type Culture Collection and maintained in Dulbecco's modified Eagle's medium (DMEM)–F12 (Invitrogen, Carlsbad, CA) supplemented with 10% fetal bovine serum (Invitrogen) and 2 mM L-glutamine.

Construction of retroviral cDNA expression library. Total RNA extracted from MiaPaCa-2 cells with the use of an RNeasy Mini column and RNase-free DNase (Qiagen, Valencia, CA) was subjected to first-strand cDNA synthesis with PowerScript reverse transcriptase, SMART IIA oligonucleotide, and CDS primer IIA (Clontech, Palo Alto, CA). The resulting cDNAs were amplified for 14 cycles with 5′ PCR primer IIA and a SMART PCR cDNA synthesis kit (Clontech), with the exception that LA *Taq* polymerase (Takara Bio, Shiga, Japan) was substituted for the Advantage 2 DNA polymerase provided with the kit. The amplified cDNAs were treated with proteinase K, rendered blunt-ended with T4 DNA polymerase, and ligated to the BstXI-adaptor (Invitrogen). Unbound adaptors were removed with the use of a cDNA size-fractionation column (Invitrogen), and the remaining cDNAs were ligated into the BstXI site of the pMXS retroviral plasmid (kindly provided by T. Kitamura, Institute of Medical Science, University of Tokyo). The resulting pMXS-cDNA plasmids were introduced into ElecroMax DH10B cells (Invitrogen) by electroporation.

Focus formation assay. BOSC23 cells (1.8×10^6) were seeded into a 6-cm culture dish, cultured for 24 h, and then transfected with 2 μg of retroviral plasmids mixed with 0.5 μg of pGP plasmid (Takara Bio), 0.5 μg of pE-eco plasmid (Takara Bio), and 18 μl of Lipofectamine reagent (Invitrogen). Two days after transfection, polybrene (Sigma, St. Louis, MO) was added to the culture supernatant at a concentration of 4 μg/ml, and the supernatant was subsequently used to infect 3T3 cells for 48 h. The culture medium of the 3T3 cells was then changed to DMEM-F12 supplemented with 5% calf serum and 2 mM L-glutamine, and the cells were cultured for 2 weeks.

Recovery of cDNAs from transformants. Transformed 3T3 cell clones were harvested with a cloning syringe and cultured independently in 10-cm culture dishes. Genomic DNA was extracted from each clone by standard procedures and then subjected to PCR with 5′ PCR primer IIA and LA *Taq* polymerase for 50 cycles of 98 °C for 20 s and 68 °C for 6 min. Amplified DNA fragments were purified by gel electrophoresis and ligated into the pT7Blue-2 vector (EMD Biosciences, San Diego, CA) for nucleotide sequencing.

Anchorage-independent growth in soft agar. 3T3 cells (2×10^6) were infected with a retrovirus encoding a truncated form of LTBR or activated KRAS2 (see Results), resuspended in the culture medium supplemented with 0.4% agar [SeaPlaque GTG agarose (Cambrex, East Rutherford, NJ)], and seeded onto a base layer of complete medium supplemented with 0.5% agar. Cell growth was assessed after culture for 2 weeks.

Tumorigenicity assay in nude mice. 3T3 cells (2×10^6) infected with a retrovirus either encoding the truncated form of LTBR or containing the human wild-type LTBR cDNA (GeneCopoeia, Germantown, MD) were resuspended in 500 μl of phosphate-buffered saline and injected into each shoulder of a nu/nu Balb-c mouse (6-weeks old). Tumor formation was assessed after 3 weeks.

5′-Rapid amplification of cDNA ends (RACE). 5′-RACE was performed as described [8]. In brief, total RNA extracted from MiaPaCa-2 cells was used to generate cDNAs with an LTBR-specific primer (5′-GCAGTGGCTGTACCAAGTCA-3′). Excess primer was removed with a microconcentrator (Amicon, Austin, TX), and a poly(A) tail was added to the cDNAs by incubation with dATP and terminal deoxynucleotidyl-transferase (Invitrogen). The first PCR was performed with the dT-adaptor primer (5′-GACTCGAGTCGACATCGATTTTTTTTTTTTT TTTT-3′) and RACE-1 antisense primer (5′-CTCCCAGCTTCCAGCT ACAG-3′), and the second PCR with the adaptor primer (5′-GACTCGA GTCGACATCG-3) and RACE-2 antisense primer (5′-GAGCAGAAA GAAGGCCAGTG-3′). The amplification protocol for the first PCR comprised incubation at 94 °C for 2 min followed by 20 cycles of 94 °C for 1 min, 55 °C for 1 min, and 72 °C for 3 min. That for the second PCR included incubation at 94 °C for 2 min followed by 30 cycles of 94 °C for 1 min, 53 °C for 1 min, and 72 °C for 3 min.The final PCR products were ligated into pT7Blue-2 for nucleotide sequencing.

Results

Screening for transforming genes by focus formation assay

To screen for transforming genes in PDC, we constructed a cDNA expression library from MiaPaCa-2 cells. Full-length cDNAs were selectively amplified by a PCR protocol from total RNA isolated from the cells and were ligated into the retroviral vector pMXS. We obtained a total of 1.2×10^6 colony-forming units of independent library clones, from which we randomly selected 30 clones and examined the incorporated cDNAs. An insert of $\geqslant$500 bp was present in 24 (80%) of the 30 clones and the average size of these 24 inserts was 1.84 kbp.

Introduction of the library plasmids into a packaging cell line yielded a recombinant retroviral library that was used to infect mouse NIH 3T3 fibroblasts. After culture of the infected cells for 2 weeks, a total of 18 transformed foci were identified. No foci were observed for 3T3 cells infected with the empty virus. Each transformed focus was isolated, expanded, and used to prepare genomic DNA. PCR amplification of the inserts identified a total of 29 cDNA fragments, each of which was ligated into a cloning vector and subjected to nucleotide sequencing from both ends. Screening of the 29 cDNA sequences against the public nucleotide sequence databases revealed that they showed >95% sequence identity to 13 independent genes, 11 known and 2 unknown (Table 1).

To confirm the transforming ability of the isolated cDNAs, we again ligated them into pMXS and used the corresponding retroviral vectors to re-infect 3T3 cells. Two of the 13 independent genes (clone ID #4, corresponding to *LTBR* [GenBank Accession No. NM_002342]; clone ID #10, corresponding to *KRAS2* [GenBank Accession No. NM_004985]) reproducibly induced the formation of transformed foci in 3T3 cells (Fig. 1). Further sequencing our *KRAS2* cDNA revealed that it has a point mutation leading to the amino acid change from a glycine residue at position 12 to a cysteine (data not shown). Whereas the oncogenic potential of mutated *KRAS2* has been